In vivo Micro PIV in the Embryonic Avian Heart

P. Vennemann, K. T. Kiger, N. T. C. Ursem, T. L. M. ten Hagen, S. Stekelenburg-de Vos,
B. C. W. Groenendijk, R. Lindken, R. E. Poelmann, J. Westerweel, B. P. Hierck,

Abstract A micro-Particle Image Velocimetry (µPIV) system is utilized for *in vivo* PIV in the heart of a chicken embryo. Long circulating, fluorescent lipid micro-spheres serve as tracer particles. The measurement system is triggered by the heart beat of the embryo to allow the collection of phase locked image ensembles. The velocity distribution in the developing ventricle is resolved at different stages within the cardiac cycle. Peak velocities of 26 mm/s are measured. The measured velocity distribution is compared with gene expression patterns.

1 Motivation

The measurement of spatial velocity fields is required for determining hydrodynamic wall shear stresses on the surface of moving boundaries such as those found in the heart. Experimental values for the wall shear stress, τ, can be extracted from the velocity field by the calculation of the velocity gradient perpendicular to the wall, $\partial u/\partial n$:

$$\tau = \eta \cdot \partial u / \partial n \tag{1}$$

where η is the dynamic viscosity of the fluid.

The wall shear stress is an important parameter in fundamental areas of angiogenesis and cardiology and plays a key role in the study of cardiogenesis (Hove *et al.* (2003), Hogers *et al.* (1999)). Placental blood flow is expected to play a significant role in normal and abnormal human heart development. For studying this relationship experimentally, an embryonic chicken model is used (Figure 1). On the right and left side of the embryo one can see vitelline vessels. The function of these vessels is comparable to the embryonic blood vessels of the mammalian placenta. It has been shown that obstructing venous flow by closing one of the vitelline veins with a clip results in severe cardiovascular malformations (Hogers *et al.* (1999)). It is speculated that the development is strongly linked to specific details of the wall shear stress patterns within the forming heart. From *in vitro* flow studies on the vascular endothelium, it is known that flow induced shear stress modulates gene expression (Topper *et al.* (1999)). *In vivo* analysis of the intracardiac flow of a zebra fish reveals shear forces being a key factor in the embryonic cardiogenesis (Hove *et al.* (2003)).

Advantageous for determining wall shear stress is the fact that the implementation of PIV also allows for a precise determination of the flow boundary. This holds in particular for situations where the boundary is not stationary, like in the case of a beating heart. Such measurements would be impracticable with single point-measurement techniques. By comparing the fluorescent visualization of gene expression with a quantitative measurement of the instantaneous flow field *in vivo* using PIV, a relationship between abnormal placental blood flow and cardiovascular malformations might be found.

2 Materials and Methods

Due to the dimensions of the embryonic chicken heart (about 200 µm inner diameter) a µPIV system is utilized (Santiago *et al.* (1998), Meinhart *et al.* (1999)). Several authors have demonstrated the applicability of µPIV or

P. Vennemann, R. Lindken, J. Westerweel
Laboratory for Aero- and Hydrodynamics, Delft Technical University, Delft, 2628CA, The Netherlands
K. T. Kiger,
Department of Mechanical Engineering, University of Maryland, College Park, MD, 20742, USA
N. T. C. Ursem, S. Stekelenburg-de Vos,
Department of Obstetrics and Gynaecology, Erasmus Medical Center, Rotterdam, 3000CA, The Netherlands
B. C. W. Groenendijk, R. E. Poelmann, B. P. Hierck,
Department of Anatomy and Embryology, Leiden University Medical Center, Leiden, 2300RC, The Netherlands
T. L. M. ten Hagen
Department of Surgical Oncology, Erasmus Medical Center, Rotterdam, 3000CA, The Netherlands

Correspondence to:
P. Vennemann, Laboratory for Aero- and Hydrodynamics, Delft Technical University, Leeghwaterstraat 21, Delft, 2628CA, The Netherlands
E-mail: p.vennemann@wbmt.tudelft.nl

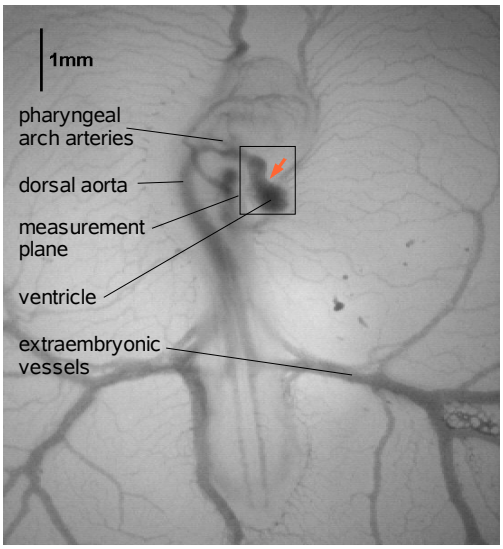

Figure 1: Chicken embryo after approximately 55 hours of incubation. The extraembryonic vessels (vitelline vessels) serve the same function as the embryonic, placental vessels of a mammalian embryo.

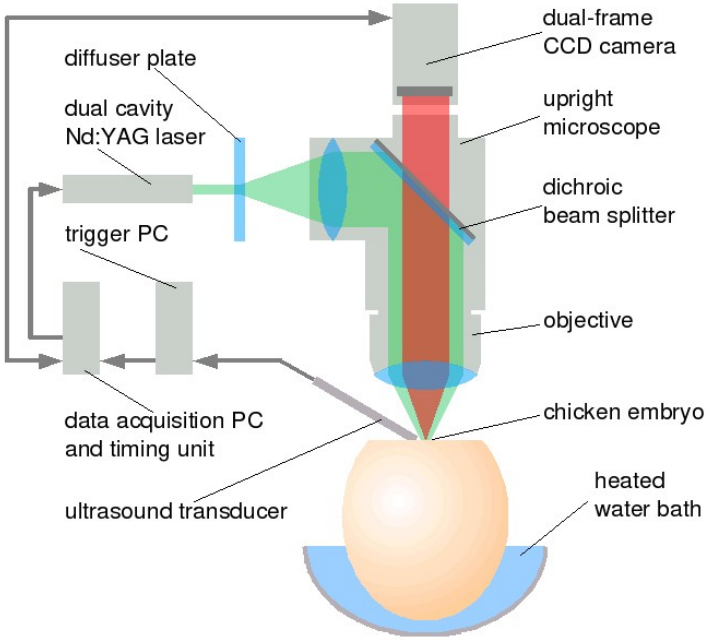

Figure 2: Schematic overview of the experimental set-up.

related techniques to study blood flow. Tangelder *et al.* (1986) labelled blood platelets with a fluorescent dye to measure steady flow velocities in arterioles of the rabbit mesentery by determining the velocity of individual particles. Individual velocity measurements at different radial positions of the blood vessel were assembled to estimate the velocity profile. Smith *et al.* (2003) refined this method by injecting fluorescent microspheres (500 nm diameter) into the mouse cremaster muscle venules. Hitt *et al.* (1996) applied a correlation technique to video images of the venous flow of red blood cells in the hamster cremaster muscle. Tsukada *et al.* (2000) and Sugii *et al.* (2002) used PIV to measure red blood cell velocity profiles in mesentery vessels of rats. Hove *et al.* (2003) followed the course of small groups of erythrocytes through the heart of a zebrafish embryo.

In contrast to red blood cells (that have a diameter of about eight micrometers) small, artificial tracer particles can enhance resolution and reliability of the measurement significantly. Accordingly the present work focuses on the use of rhodamine tagged, polyethylene glycol (PEG) coated, lipid-microspheres as long circulating tracer particles. The nominal diameter of the particles is 400 nm, although agglomerates were also observed. Fluorescence based imaging enables the distinction between background light that is scattered by blood cells and tissue, and the signal coming from the tracer particles.

Fertilized White Leghorn eggs were incubated until they reach development Stage 15 (according to the staging criteria of Hamburger and Hamilton (1951) (see Figure 1). Part of the egg shell is removed to establish optical access to the embryo. To prevent desiccation by evaporation, the opening is covered with a film of purified mineral oil. To maintain a constant temperature of 37 degrees Celsius the egg is partially immersed in a constant temperature water bath during the experiment. Figure 2 schematically shows the experimental set-up. It mainly consists of a fluorescence microscope with a dual-cavity Nd:YAG laser (frequency doubled) and a dual-frame CCD camera. Laser and camera are synchronized by a timing unit built into a PC. Figure 2 further shows an ultrasound Doppler velocimeter and an additional PC to trigger the timing unit with the heartbeat of the embryo. This is to provide time-resolved ensemble average measurements throughout the cardiac cycle. The blood flow is observed through a 10× magnification apochromatic objective with an numerical aperture, NA, of 0.4. The microscope is equipped with a dichroic mirror suitable for 532 nm excitation and 560 nm peak emission wavelength. The laser is operated at approximately 0.5 mJ light energy per pulse. To attenuate speckle noise a 10 degree light shaping diffuser is mounted into the light path. For the synchronization of the data-acquisition PC to the cardiac cycle of the chicken embryo, the acoustic probe of a 20-MHz ultrasound pulsed Doppler velocimeter is placed close to the dorsal aorta of the embryo.

The tracer particles are injected into one of the vitelline veins using an approximately 10 µm thick glass-pipette. The PEG-coating prevents the particles from adhering to the walls of the vasculature. The liposomes are biodegradable and can therefore be used in non-final animal experiments (Woodle (1992)).

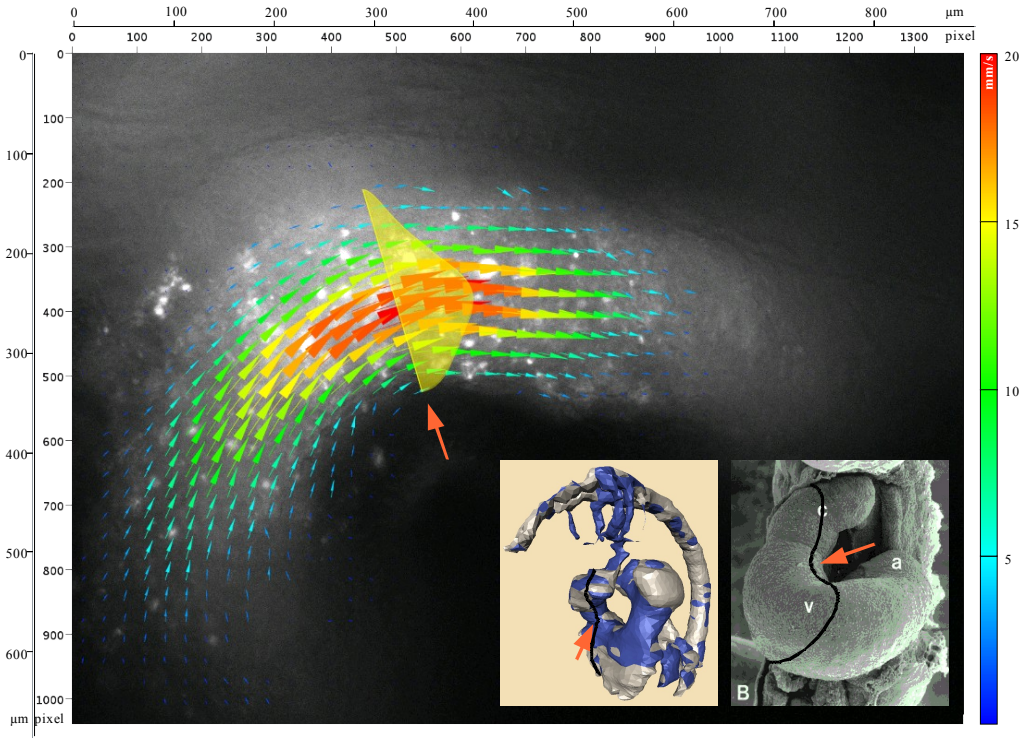

Figure 3: PIV measurement in the developing ventricle of a chicken embryo. The left inset shows the expression of KLF-2 in a chicken heart of the same age (Groenendijk *et al.* (2004)). In the scanning electron micrograph from Männer (2000) the location and spatial orientation of the measurement plane is indicated.

3 Results and Discussion

Measurements are made at different points in the cardiac cycle. Each measurement represents the ensemble averaged evaluation of fifty image pairs with an interframing time of 0.5 to 4 ms, depending on the average magnitude of the velocities at a given point in the cycle.

Figure 3 shows the average of fifty phase-locked vector fields in the fully expanded ventricle. The flow enters from the left side of the image where the blood emerges perpendicular to the image plane. After crossing the image plane, the flow disappears again normal to the image plane in the direction of the arteries. The corresponding Reynolds number is about 0.5 at this point of the cardiac cycle. The Womersley number for the adjacent arteries is of order 0.2. Only the velocity components parallel to the image sensor are measured. This explains the decrease of velocity magnitude at the left and the right side of the flow field. At the cross section indicated by the orange arrow, the flow is assumed to be parallel to the image plane. For comparison, the approximately same position in the insets is also indicated by arrows. The third velocity component is assumed to be zero at this cross section. At this position a single velocity profile is superimposed as a continuous curve (yellow). The profile shows an asymmetrical velocity distribution. This suggests the highest shear stress will appear at the inner curvature. The relatively large interrogation windows of 64 × 64 pixels lead to an overestimate of the near-wall velocity when the interrogation region partially extends out of the flow region. Under such circumstances, the estimated velocity equals the average velocity of the particle-containing region of the window. This effect is accounted for by omitting the affected vectors during the interpolation of the velocity profile.

For the case shown in Figure 3, this results in a maximum strain rate of 1×10^{3} s^{-1} on the higher curvature wall. In comparison, the human vascular network experiences wall shear stress values up to approximately 7 Pa (Malek *et al.* 1999). In the current estimate, a minimal value of the viscosity was assumed (corresponding to a magnitude slightly greater than that of clear plasma) in order to provide a conservative estimate of the wall shear stress. The non-Newtonian behavior of blood is less critical at shear rates that are relevant for the present study. Measurements from Chien (1970) show that at a shear rate above 1×10^{2} s^{-1} neither aggregation occurs, nor can the deformability of the erythrocytes further decrease the viscosity. Therefore the effective viscosity remains constant so that in this par-

ticular case the non-Newtonian behavior of blood can be ignored. Groenendijk *et al.* (2004) visualized the shear dependent production of KLF-2 in the cardiovascular system of chicken embryos (Figure 3, left inset). The production of KLF-2 is known to be upregulated at higher shear stress . In agreement with the measured velocity profile, the left inset of Figure 3 shows high levels of KLF-2 (blue) at the inner curvature of the heart.

In the present measurements we encountered a broad size distribution of the tracer particles. In future work, improving the control of the tracer particle size will have benefits:

1) Uniformly sized particles will allow for a higher number concentration for the same volume fraction of tracer particles and a much smaller interrogation window, increasing the spatial resolution;

2) The absence of large particles will also help minimize the effective depth of focus of the measurement plane.

At a magnification of 20× (instead of 10× at present) and by reducing the interrogation window size to 32 pixels (instead of 64 pixels), a resolution of 10 µm × 10 µm × approximately 7 µm (depth of correlation, Olsen *et al.* (2000)) is feasible.

4
Acknowledgements

This project is funded by the Dutch Technology Foundation STW (DSF.5695), the Netherlands Heart Foundation (NHF 2000.016; BPH, SS, BCWG), and the Dutch Cancer Foundation (DDHK2000-2224).

References

Chien S (1970) Shear dependence of effective cell volume as a determinant of blood viscosity. Science 168, 977-979.

Groenendijk B C; Hierck B P; Gittenberger-de Groot A C; Poelmann R E (2004) Development-related changes in the expression of shear stress responsive genes KLF-2, ET-1, and NOS-3 in the developing cardiovascular system of chicken embryos. Developmental Dynamics 230 (1), 57-68.

Hamburger V; Hamilton H (1951) A series of normal stages in the development of the chick embryo. Journal of Morphology 88, 49-92.

Hitt D; Lowe M; Tincher J; Watters J (1996) A new method for blood velocimetry in the microcirculation. Microcirculation 3 (3), 259-263.

Hogers B; DeRuiter M C; Gittenberger-de Groot A C; Poelmann R E (1999) Extraembryonic venous obstructions lead to cardiovascular malformations and can be embryolethal. Cardiovascular Research 41, 87-99.

Hove J R; Köster R W; Forouhar A S; Acevedo-Bolton G; Fraser S E; Gharib M (2003) Intracardiac fluid forces are an essential epigenetic factor for embryonic cardiogenesis. Nature 421, 172-177.

Malek A; Alper S; Izumo S (1999) Hemodynamic shear stress and its role in atherosclerosis. JAMA 282, 2035-2042.

Männer J (2000) Cardiac looping in the chick embryo: A morphological review with special reference to terminological and biomechanical aspects of the looping process. The Anatomical Record 259, 248-262.

Meinhart C D; Wereley S T; Santiago J G (1999) PIV measurements of a microchannel flow. Experiments in Fluids 27, 414-419.

Olsen M; Adrian R (2000) Out-of-focus effects on particle image visibility and correlation in microscopic particle image velocimetry. Experiments in Fluids 29 (Suppl. 7), 166-174.

Santiago J; Wereley S; Meinhart C; Beebe D; Adrian R (1998) A particle image velocimetry system for microfluidics. Experiments in Fluids 25, 316-319.

Smith M; Long D; Damiano E; Ley K (2003) Near-wall µPIV reveals a hydrodynamically relevant endothelial surface layer in venulus *in vivo*. Biophysical Journal 85, 637-645.

Sugii Y; Nishio S; Okamoto K (2002). Measurement of a velocity field in microvessels using a high resolution PIV technique. Annals of the New York Academy of Sciences 972, 331-336.

Sugii Y; Nishio S; Okamoto K (2002). In vivo PIV measurements of red blood cell velocity field in microvessels considering mesentery motion. Physiological Measurement 23, 403-416.

Tangelder G; Slaaf D; Muijtjens A; Arts T; oude Egbrink M; Reneman R (1986) Velocity profiles of blood platelets and red blood cells flowing in arterioles of the rabbit mesentery. Circulation Research 59 (5), 505-514.

Topper J N; Gimbrone Jr M A (1999) 1999. Blood flow and vascular gene expression: fluid shear stress as a modulator of endothelial phenotype. Molecular Medicine Today 5 (1), 40-46.

Tsukada K; Minamitani H; Sekizuka E; Oshio C (2000) Image correlation method for measuring blood flow velocity in microcirculation: correlation 'window' simulation and in vivo image analysis. Physiological Measurement 21, 459-471.

Woodle M; Lasic D (1992) Sterically stabilized liposomes. Biochimica et Biophysica Acta 1113 (2), 171-199.